

Thermal decomposition and kinetics studies on 1,4-dinitropiperazine (DNP)

Yan Qi-Long^{a,*}, Li Xiao-Jiang^a, Wang Han^a, Nie Li-Hua^b, Zhang Ze-Yi^a, Gao Hong-Xu^a

^a Xi'an Modern Chemistry Research Institute, Xi'an 710065, China

^b Department of Material Science & Engineering, Xi'an University of Science & Technology, Xi'an 710054, China

Received 22 March 2007; received in revised form 4 June 2007; accepted 6 June 2007

Available online 12 June 2007

Abstract

DNP, a nitramine, has been studied with regard to the kinetics and mechanism of thermal decomposition, using thermogravimetry (TG), differential thermal analysis (DTA), infrared (IR) spectroscopy, and differential scanning calorimetry (DSC). The IR spectra of DNP have also been recorded and the kinetics of thermolysis has been followed by non-isothermal TG. The activation energy of the solid-state process was determined using Flynn–Wall–Ozawa method. The actual reaction mechanism obeyed nucleation and growth model, Avrami Erofeev function ($n = 1$) with integral form $G(\alpha) = -\ln(1 - \alpha)$ ($\alpha = 0.10$ – 0.65). E_a and A were determined to be 116.51 kJ/mol and $10^{10.52} \text{ s}^{-1}$. The T/Jump FT-IR analysis showed that CH_2O , NO_2 , and NO are produced in larger amounts than CO_2 and HCN . The cleavage of the N–N and C–N bond appears to be the primary step in the thermolysis of DNP.

© 2007 Elsevier B.V. All rights reserved.

Keywords: Kinetics; Mechanism; Decomposition; TG; DSC

1. Introduction

Development of energetic materials with improved combustion properties and low sensitivity is underway to meet superior performance requirements, and they appear to be the future candidates to compete with the currently used high performance high energy materials such as cyclotrimethylenetrinitramine (RDX) and cyclotetramethylenetetranitramine (HMX) [1,2]. However, 1,4-dinitropiperazine (DNP) is an energy compound of this kind [3–5].

Thermoanalysis is the best way of studying energetic materials, so the investigation on decomposition of energetic materials was vastly carried out by scientists all over the world. It is reported that there is a strong dependence between pressure and the thermal decomposition [6,7] and the heat of combustion of DNP is 15.2 kJ g^{-1} . It is also reported that the shock sensitivity of this kind of compound is related to the bond strength of the nitramino group [8,9]. Yinon [10], using MS/MS collision induced dissociation studies, was able to show the fragmentation process and paths in a series of commonly used energetic

materials which included nitramines. Nikishev et al. [11] are of the opinion that the reactivity of the nitramines in homolytic thermoanalysis is governed by the closeness of the electronic structure of the reaction centre in ground and transition states. Sitonina et al. [12] did research on the kinetics of the thermal decomposition of *N,N'*-dinitropiperazine and 1,3-dinitro-1,3-diazacyclopentane. It is reported that the activation parameters for the thermal decomposition of the cyclic nitroamines are only weakly dependent on the number of nitroamine groups in the molecule, and the size of the ring. However no data are available regarding the kinetics and mechanism of the thermal decomposition of this compound or its structural aspects, so the present paper is an effort to increase our knowledge in this direction.

2. Experimental

DNP (99.8%) was synthesized by our work group, and it was studied with regard to the kinetics and mechanism of thermal decomposition, using thermogravimetry (TG), differential thermal analysis (DTA), infrared (IR) spectroscopy, and differential scanning calorimetry (DSC). The IR series spectra of DNP have also been recorded and the bands assigned. The kinetics of thermolysis has been followed by isothermal TG.

* Corresponding author. Tel.: +86 29 88294031.
E-mail address: terry.well@163.com (Q.-L. Yan).

The original T/Jump FT-IR instrument was used with the data collection rate of 1.8988 cm s^{-1} and differentiating rate is 4 cm^{-1} . The PDSC (TA910s, made in America) instrument was introduced in the static nitrogen atmosphere, and the pressure was 0.1 MPa, 2 MPa, 4 MPa, 6 MPa. The sample quantum was about 1.5 mg, and the heating rate is about $10^\circ\text{C min}^{-1}$. TG (TA2950) instrument provided by Nicolet Company worked in a temperature range of $15\text{--}300^\circ\text{C}$, and the heating rate was $2.5^\circ\text{C min}^{-1}$, 5°C min^{-1} , $10^\circ\text{C min}^{-1}$, $20^\circ\text{C min}^{-1}$ when the sample quantum was about 1.5 mg and with dynamic nitrogen atmosphere.

3. Results and discussions

3.1. IR studies

The research of this aspect was also carried out by Peiris et al. [13] and the IR spectra of DNP are in agreement with their experiment result. The symmetric nitro stretching modes are multiplets. The N–NO₂ band can easily be identified by its characteristic stretching absorption at 1557 cm^{-1} . The CH₂ scissoring modes are unusually weak at $1410\text{--}1460 \text{ cm}^{-1}$ although the CH₂ wagging modes are fairly strong, and its wavenumber was influenced by water and carbon dioxide in the air.

3.2. TG/DTG studies

TG curves of DNP (Fig. 1) were recorded under different conditions. The TG of DNP in static air at a heating rate of $2.5^\circ\text{C min}^{-1}$ showed a sharp change in mass of 75% followed by a very slow change in mass of 17%. These mass changes occurred in the temperature ranges $160\text{--}220^\circ\text{C}$ and $220\text{--}280^\circ\text{C}$, respectively. The results obtained were similar when the heating rate (β) was changed to 5°C min^{-1} , $10^\circ\text{C min}^{-1}$ or $20^\circ\text{C min}^{-1}$. When the heating rate was changed to $20^\circ\text{C min}^{-1}$, the initial mass loss was observed at the lower temperature ranges of $150\text{--}205^\circ\text{C}$. Respectively, DTG of DNP (Fig. 2) showed a sharp maximum decomposition rate in the temperature of 205.3°C , 220.5°C , 225.6°C and 245.8°C at

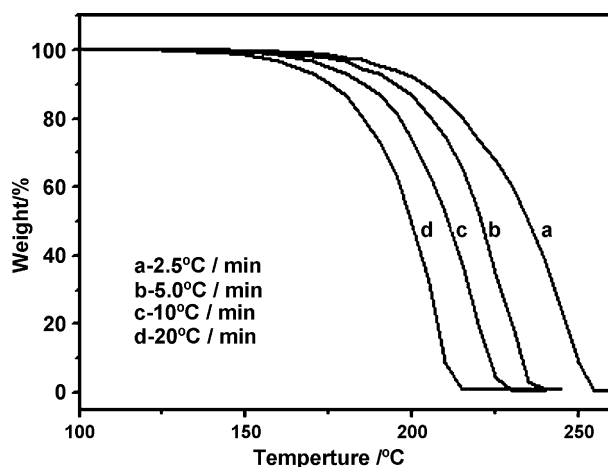


Fig. 1. TG curves of DNP with different heating rates.

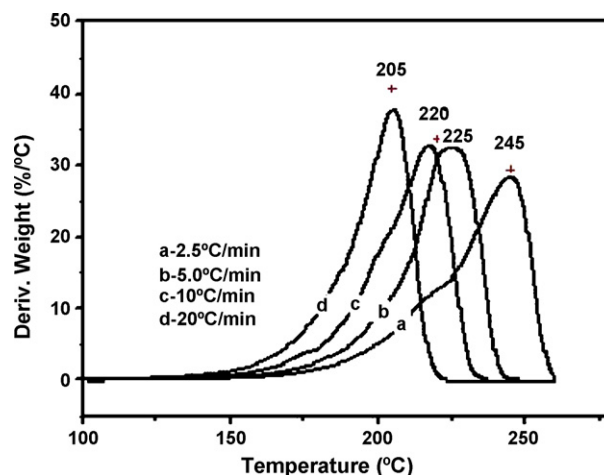


Fig. 2. DTG curves of DNP with different heating rates.

a heating rate of $2.5^\circ\text{C min}^{-1}$, 5°C min^{-1} , $10^\circ\text{C min}^{-1}$ and $20^\circ\text{C min}^{-1}$ in static air. With the heating rate increased, the weight loss rate per degree centigrade was decreased while rate per minute was enlarged. The maximum decomposition rate per degree centigrade was $2.5 \times 4 = 4.0\%^\circ\text{C}^{-1}$ with the β of $2.5^\circ\text{C min}^{-1}$, and the maximum decomposition rate per minute was $3.0 \times 20 = 60\% \text{ min}^{-1}$ with the β of $20^\circ\text{C min}^{-1}$. It was concluded that the decomposition reaction time reduced when β increased.

3.3. PDSC studies

TG/DTG data were supplemented by DSC studies at a heating rate of $10^\circ\text{C min}^{-1}$. When the pressure is 2 MPa, the DSC trace (Fig. 3) obtained with the sample encapsulated in an aluminium cup showed a sharp exothermic change. The onset of the exotherms was noticed at 251.2°C with the peak maximum at 283.1°C . This exothermic change was covered by an energy change of 1346.2 J g^{-1} . The fact that DSC curves showed a sharp endothermic change before the onset of exothermic change indicated that the compound melted before decomposed. When the pressure is 0.1 MPa, there was no exothermic but a sharp

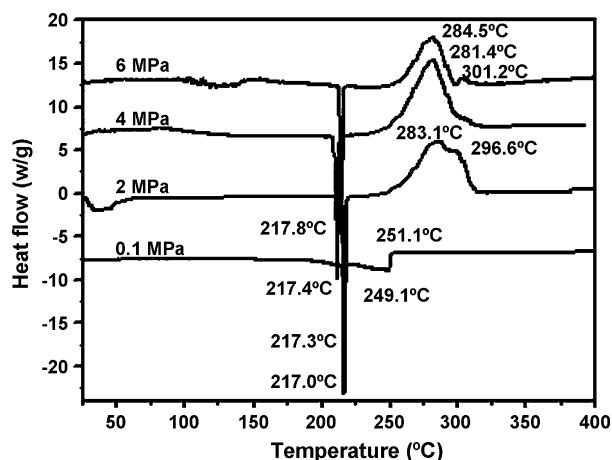


Fig. 3. DSC curves of DNP in different pressure.

Table 1

The kinetics parameters of DNP by Flynn–Wall–Ozawa method from data of multi-heating rate non-isothermal TG experiments

α	Heating rate (°C/min)				E_a (kJ mol ⁻¹)	log A (s ⁻¹)	r
	2.5	5	10	20			
0.05	165.59	175.16	184.43	192.36	124.59	11.39	0.9982
0.1	175.36	185.62	195.25	203.24	124.98	11.41	0.9974
0.15	181.32	191.39	201.46	210.24	124.10	11.30	0.9988
0.20	185.43	196.03	205.87	215.15	123.73	11.26	0.9988
0.25	188.88	199.39	209.69	219.24	122.83	11.16	0.9992
0.30	191.70	201.75	212.81	223.20	119.76	10.84	0.9998
0.35	194.36	204.26	215.32	226.87	117.94	10.62	0.9999
0.40	196.07	206.76	217.52	229.97	114.99	10.31	0.9998
0.45	198.29	208.96	219.39	232.63	114.99	10.31	0.9993
0.50	199.65	210.90	220.74	235.12	112.82	10.10	0.9980
0.55	201.32	212.64	222.00	237.29	112.34	10.06	0.9965
0.60	202.80	214.25	223.37	239.20	111.88	10.03	0.9955
0.65	204.15	215.78	224.96	241.06	111.08	9.97	0.9953
0.70	205.49	217.21	226.64	242.90	110.23	9.90	0.9956
0.75	206.75	218.62	228.28	244.65	109.44	9.84	0.9960
0.80	207.89	220.02	229.88	246.36	108.44	9.76	0.9962
Mean					116.51	10.52	0.9978

endothermic change. This indicated that the sample melted and volatilized without decomposition in normal air pressure.

When the pressure increased, the position of endothermic change did not vary essentially, but the exothermic peak temperature changed a lot. Besides the main exothermic peak, there was a lower exothermic peak. This became more evidently when the pressure increased. This can account for that after the initial cleavage the specified the secondary reactions took place. Further more, we can also conclude that DNP thermal decomposition process contained one main and another very slow stage. The decomposition involves about 92% loss in mass in the ranges 150–220 °C and 220–302 °C. The DSC curves show two exothermic changes. Except for 0.1 MPa, decomposition of DNP had taken place and the exothermic peak changed a lot with the pressure alternated.

3.4. Thermal decomposition kinetics

The kinetics of the thermal decomposition of DNP at different temperatures in the range 185–200 °C under static air were studied by non-isothermal TG. From data of the non-isothermal TG experiments (Table 1) the mass loss with respect to temperature was noted. In order to obtain the value of two kinetic parameters [apparent activation energy (E_a) and pre-exponential factor (A)] of the major exothermic decomposition reaction for DNP, the multiple heating-rate method proposed by Flynn–Wall–Ozawa [14,15] used the following approximate equation at a constant weight loss in a thermal degradation process:

$$\log[\beta] = \log\left(\frac{AE_a}{R}\right) - \log F(\alpha) - 2.315 - \frac{0.4567E_a}{RT}$$

where β is the heating rate in the non-isothermal TG measurement. From this equation E_a can easily be calculated based on the slope of a plot of $\log(\beta)$ versus $1/T$ at a fixed weight loss. The Flynn–Wall–Ozawa method is the most useful method for

the kinetic interpretation of the thermogravimetric data obtained when studying complex processes. This method can determine the activation energy without knowledge of reaction order.

The E_a of thermal degradation for DNP was obtained by the Ozawa method, from a linear fitting of $\log(\beta)$ versus $1000/T$ at a fixed conversion with the slope of such a line being $-0.4567E_a/RT$. For this study, the conversion values are 0.10, 0.20, 0.30, 0.40, 0.50, and 0.60. Fig. 4 shows that the fitting straight lines are nearly parallel, which indicates that this method is applicable to our system in the conversion range studied. This fact suggests that a single reaction mechanism is operative. The activation energies calculated from the slopes corresponding to the different conversions are shown in Fig. 5. From these values a mean E_a value of 116.51 kJ/mol was found.

Fig. 5 shows the variation of the activation energy with the conversion degree, suggesting successive reactions. It illustrates the relationship between the activation energies of the

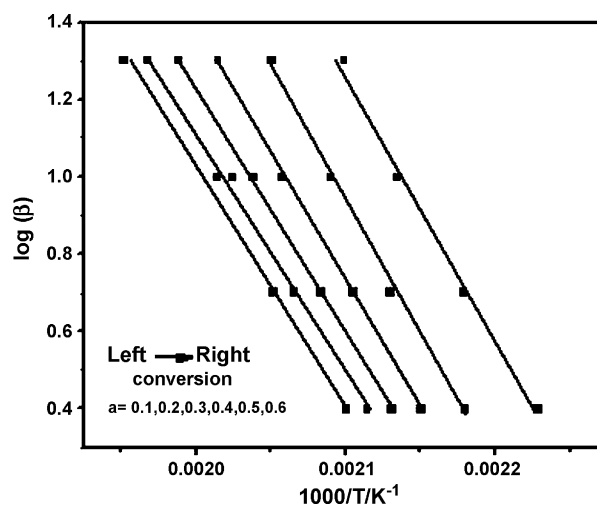


Fig. 4. Flynn–Wall–Ozawa plots at varying conversion for the degradation.

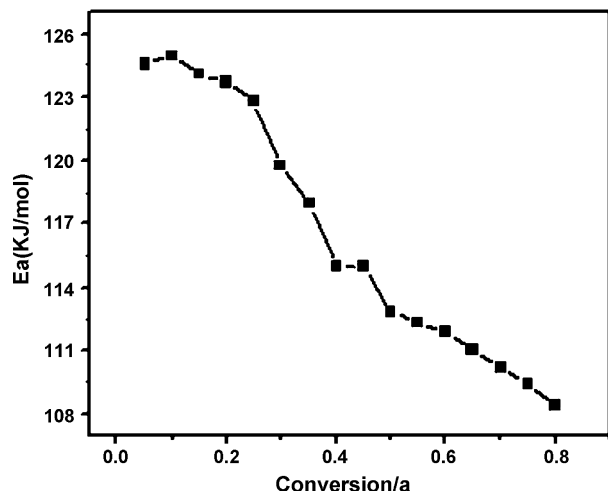


Fig. 5. Dependence of the apparent activation energy on the degree of conversion determined using isoconversional method for the non-isothermal TG data (open circles: $\beta = 2.5$ K/min, 5 K/min, 10 K/min and 20 K/min).

degree of conversion, due to continuous change of decomposition mechanisms. Vyazovkin and Wight [16] have reported that concentration of nuclei at fast heating rate, which is commonly the case for isothermal system, is very low and the isothermal decomposition is limited by nucleation only. But in case of non-isothermal decomposition, it is limited by nuclei growth since the heating rate is low ($2.5\text{--}20$ K min^{-1} in the present case). They also added that nucleation and nuclei growth takes place at lower and higher activation energies, respectively. Therefore, we may find decrease activation energies for non-isothermal cases, respectively. In addition, it is also reported by Vyazovkin and Wight [16], Vyazovkin [17] that diffusion of the formed gas plays an important role to reduce the activation energy in the subsequent stages of the decomposition phenomenon. Therefore in

case of non-isothermal decomposition, the two opposite effects (nuclei growth and gas diffusion) may finally make activation energy a weak function of conversion. The activation energy quickly falls with conversion. This may possibly be attributed to the fact that at the later stage formation of porous solid residue makes the diffusion faster leading to more decrease in activation energy.

In order to make a comparison and reduce the kinetic model function $f(\alpha)$, the integral equations (1)–(3) are cited to obtain the values of E_a , and A from a single non-isothermal TG curves [18].

$$\lg[G(\alpha)] = \lg\left(\frac{AE_a}{\beta R}\right) - 0.4828E_a^{0.4357} - \left(\frac{0.449 + 0.217E_a}{0.001T}\right) \quad (1)$$

$$\lg[G(\alpha)] = \lg\left(\frac{AE_a}{\beta R}\right) - 2.315 - \frac{0.4567E_a}{RT} \quad (2)$$

$$\lg\left[\frac{G(\alpha)}{T^2}\right] = \ln\left\{\frac{AR}{\beta E_a}\left[\frac{1 - 2(RT/E_a)}{1 - 5(RT/E_a)}\right]\right\} - \frac{E_a}{RT} \quad (3)$$

where $f(\alpha)$ and $G(\alpha)$ are the differential and integral model functions, respectively; T_0 , the initial point at which DSC curve deviates from the baseline; R , the gas constant; α , conversion degree ($\alpha = H_t/H_0$); H_0 , the total heat effect (corresponding to the global area under the DSC curve); H_t , the reaction heat at a certain time corresponding to the partial area under the DSC curve); T , temperature (K) at time t .

Forty-one types of kinetic model functions [18] and the data in Table 2 are put into Eqs. (1)–(3) for calculation, respectively. The values of E_a , A , linear correlation coefficient (r), standard mean square deviation (Q) and believable factor (d) [where $d = (1 - \alpha)Q$] were obtained by the linear least squares and iterative methods [19]. The probable kinetic model functions of the

Table 2
Basic data of the major exothermic decomposition reaction of DNP

$\beta = 2.5$ °C min^{-1}		$\beta = 5$ °C min^{-1}		$\beta = 10$ °C min^{-1}		$\beta = 20$ °C min^{-1}	
T (°C)	α (%)	T (°C)	α (%)	T (°C)	α (%)	T (°C)	α (%)
171	6.251	190	25.85	184	7.643	203	31.75
172	6.781	191	27.68	185	8.519	204	33.68
173	7.357	192	30.38	186	9.129	205	35.67
174	7.967	193	31.98	187	9.955	206	37.67
175	8.655	194	33.54	188	10.79	207	39.78
176	9.379	195	35.69	189	11.43	208	42.05
177	10.03	196	38.68	190	12.29	209	44.45
178	10.82	197	41.35	191	13.66	210	47.00
179	11.74	198	43.56	192	14.43	211	49.69
180	12.67	199	46.85	193	15.27	212	52.56
181	13.66	200	50.34	194	16.33	213	55.55
182	14.68	201	53.44	195	17.74	214	58.71
183	15.77	202	56.74	196	19.00	215	61.95
184	16.98	203	60.21	197	20.37	216	65.38
185	18.36	204	64.04	198	22.38	217	68.88
186	20.08	205	67.78	199	23.56	218	72.45
187	21.75	206	71.60	200	25.30	219	76.15
188	23.03			201	27.44		
189	24.27			202	29.70		

Table 3
Kinetic parameters obtained by Single Heating Rate method from the TG data in Table 2*

β ($^{\circ}\text{C min}^{-1}$)	$f(\alpha)$	$G(\alpha)$	Eq. (1)		Eq. (2)		Eq. (3)	
			E_a (kJ mol^{-1})	$\lg A$ (s^{-1})	E_a (kJ mol^{-1})	$\lg A$ (s^{-1})	E_a (kJ mol^{-1})	$\lg A$ (s^{-1})
2.5	$2[1 - (1 - \alpha)^{1/2}]$	$(1 - \alpha)^{-1/2}$	115.67 ^a	12.21 ^a	117.29 ^b	12.10 ^b	115.67 ^c	11.91 ^c
5	$2[1 - (1 - \alpha)^{1/2}]$	$(1 - \alpha)^{-1/2}$	115.57 ^d	12.15 ^d	117.29 ^e	12.40 ^e	115.67 ^f	12.21 ^f
10	$2[1 - (1 - \alpha)^{1/2}]$	$(1 - \alpha)^{-1/2}$	115.57 ^g	12.45 ^g	117.29 ^h	12.71 ^h	115.67 ⁱ	12.51 ⁱ
20	$2[1 - (1 - \alpha)^{1/2}]$	$(1 - \alpha)^{-1/2}$	115.27 ^j	12.40 ^j	117.01 ^k	12.66 ^k	115.17 ^l	12.45 ^l

* ^a $r=0.9995$, $Q=1.567 \times 10^{-2}$, $d=7.395 \times 10^{-6}$; ^b $r=0.9996$, $Q=2.842 \times 10^{-3}$, $d=1.134 \times 10^{-6}$; ^c $r=0.9995$, $Q=1.567 \times 10^{-2}$, $d=7.395 \times 10^{-6}$; ^d $r=0.9996$, $Q=2.842 \times 10^{-3}$, $d=1.134 \times 10^{-6}$; ^e $r=0.9996$, $Q=2.846 \times 10^{-3}$, $d=1.134 \times 10^{-6}$; ^f $r=0.9995$, $Q=1.567 \times 10^{-2}$, $d=7.395 \times 10^{-6}$; ^g $r=0.9996$, $Q=2.842 \times 10^{-3}$, $d=1.134 \times 10^{-6}$; ^h $r=0.9996$, $Q=2.842 \times 10^{-3}$, $d=1.134 \times 10^{-6}$; ⁱ $r=0.9995$, $Q=1.567 \times 10^{-2}$, $d=7.395 \times 10^{-6}$; ^j $r=0.9987$, $Q=7.701 \times 10^{-3}$, $d=1.102 \times 10^{-5}$; ^k $r=0.9987$, $Q=7.701 \times 10^{-3}$, $d=1.102 \times 10^{-5}$; ^l $r=0.9985$, $Q=4.173 \times 10^{-2}$, $d=6.399 \times 10^{-5}$.

integral and differential methods selected by the logical choice method [20] and when $f(\alpha) = 1 - \alpha$ and $G(\alpha) = -\ln(1 - \alpha)$, the values (Table 3) obtained by Eqs. (1)–(3) are in good agreement with the calculated values obtained by Ozawa's methods ($\alpha = 0.1$ – 0.65). The results indicated that the reaction mechanism of the exothermic process of DNP ($\alpha = 0.1$ – 0.65) is classified as nucleation and nuclear growth (Avramie equation (1)) chemical reaction. Substituting $f(\alpha)$ with $1 - \alpha$, E_a with $116.51 \text{ kJ mol}^{-1}$, β with 0.1667 K s^{-1} and A with $10^{10.52} \text{ s}^{-1}$ in Eq. (4), we can establish the kinetic equation of the major exothermic decomposition process of DNP as Eq. (5).

$$\frac{d\alpha}{dt} = \frac{A}{\beta} f(\alpha) \exp\left(-\frac{E_a}{RT}\right) \quad (4)$$

$$\frac{d\alpha}{dt} = 1.802 \times 10^{10.52} (1 - \alpha) \exp\left(\frac{-0.1401 \times 10^2}{T}\right) \quad (5)$$

3.5. Thermal decomposition mechanism

The series spectra of the residue obtained in the original T/Jump FT-IR experiment showed development of bands at 1557 cm^{-1} , 1241 cm^{-1} and 2890 cm^{-1} . The observation of a large quantity of NO_2 in the evolved gas analysis and the observed preferential loss of band intensity due to the NO_2 group permits us to conclude that N–N bond cleavage may be the initial thermolysis pathway in DNP. The bands at 1334 cm^{-1} is characteristic of a C–N group and the bands at 2890 cm^{-1} is characteristic of a CH_2 group.

Oyumi and Brill [7], who have investigated the evolved gases from the thermal decomposition of TNAD, observed that considerable amounts of HONO and NO_2 are produced at lower heating rates. They further showed that the ratio of HONO/ NO_2 obtained was higher at high pressures than at low pressures. According to them, at higher pressures it is likely that the initially formed NO_2 is unable to diffuse and get engaged in further reactions with the condensed phase producing HONO, whereas at lower pressures the NO_2 cleaved can easily diffuse through. Thus the HONO formed may be due to the adventitious contact of the NO_2 formed with the ring hydrogen atom. According to Oyumi and Brill [7], in nitramines the formation of HONO is advanced with larger HONO/ NO_2 ratios and it is not a primary decomposition product, and the decomposition of DNP is similar

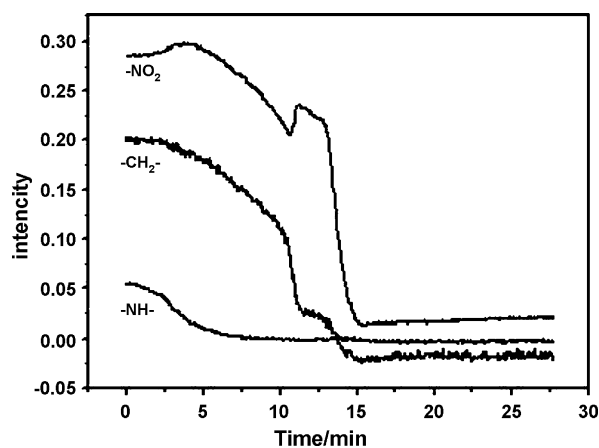


Fig. 6. The relationship between T-Jump/FT-IR absorption intensity with heating time (variety of three main IR absorption intensities).

with RDX and TNAD (*trans*-1,4,5,8-tetranitro-1,4,5,8-tetraaza docalin).

When the isothermal decomposition of DNP was followed in KBr pellet or just mixed with KBr powder it was observed that the intensity of the bands due to nitro and other groups decreased systematically (showed in Figs. 6 and 7). The loss of intensity due to nitro group was more pronounced than the intensities due to other groups. In evolved gas analysis, CH_2O , NO_2 , and NO were the major components, while CO_2 and HCN

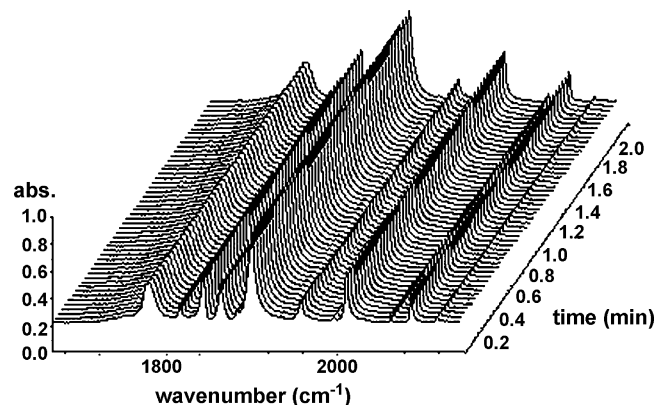


Fig. 7. The relationship between T-Jump/FT-IR absorption intensity with heating time (FT-IR spectra of gas phase decomposition of DNP).

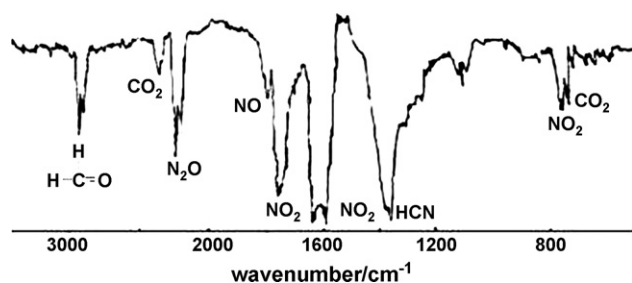
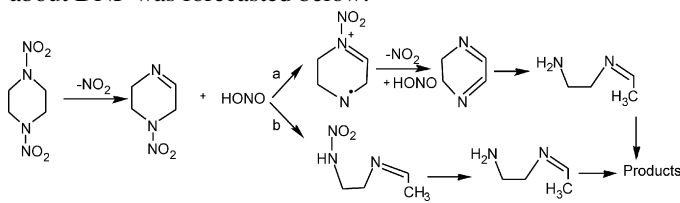


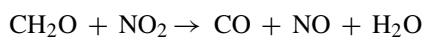
Fig. 8. IR spectra of gaseous decomposition products of DNP.

(1361 cm^{-1}) were the minor gaseous products identified by IR (Fig. 8).

Melius [20] has recently applied thermochemical model to decompositions of energetic materials and has shown that in RDX and HMX the weakest bond is N–NO₂. The bond breaking energy for this N–N bond in RDX is 205.0 kJ mol^{-1} and in HMX it is 206.0 kJ mol^{-1} , but the C–N and C–H bonds are significantly stronger. The bond breaking energies for the C–N and C–H bonds are 375.0 kJ mol^{-1} and 395.8 kJ mol^{-1} , respectively, in HMX and of similar order in RDX. However, after the rupture of the NO₂ group, the resulting second nearest neighbor bond breaking energies become very weak; for example, the C–N bond breaking energy is only 75.6 kJ mol^{-1} in HMX. Therefore in the unimolecular decomposition of RDX and HMX the order in which the bonds are broken is N–N followed by C–N. The E value [21] reported for RDX by the isothermal gas evolution method [22] is 198.6 kJ mol^{-1} (213–299 °C); from mass spectroscopic studies [23,24] it is 188.1 kJ mol^{-1} . The E value obtained in the present study suits the mechanism proposed [25,26] reasonably well and is consistent with those for RDX and HMX when the expected weaker N–N bond dissociation energy and the lower temperature of decomposition in DNP are taken into account. It is possible thereby to infer that the N–NO₂ bond cleavage is the primary step in the thermal decomposition of DNP. So the mechanism of the decomposition about DNP was forecasted below:



The magnitude of the most negative electrostatic potentials of the nitrogens can be considered to be indicative of the degrees of delocalisation of the nitrogen lone pairs, and decreases as the stability increases. In aza cyclic systems the introduction of nitro rings also has an overall stabilising effect due to further delocalisation of electrons, reflecting the strong electron withdrawing power of the nitro group. It is most likely that the mechanism suggested by Cosgrove and Owen [27] operates like a competitive secondary reaction because we have been able to detect NO as a product in evolved gas analysis. The reaction process is established below:



4. Conclusions

1. The decomposition of DNP involves about 92% loss in mass in the ranges 150–220 °C and 220–302 °C. The DSC curves show two exothermic changes. Except for 0.1 MPa, decomposition of it had taken place and the exothermic peak changed a lot with the pressure altered.
2. The activation energy of the solid-state process was determined using Flynn–Wall–Ozawa method, which does not require knowledge of the reaction mechanism, and the activation energy quickly falls with conversion. The activation energy of different mechanism models and pre-exponential factor (A) were determined by another three equations, Compared with the value obtained from the Ozawa method, the actual reaction mechanism obeyed nucleation and growth model, Avramie Erofeev function ($n=1$) with integral form $G(\alpha) = -\ln(1 - \alpha)$ ($\alpha=0.10-0.65$). Then E_a and A were determined to be 116.51 kJ/mol and 10.52. So the thermodecomposition of DNP dynamic equation is

$$\frac{d\alpha}{dt} = 1.802 \times 10^{10.52} (1 - \alpha) \exp\left(\frac{-0.1401 \times 10^2}{T}\right)$$

3. The cleavage of the N–N and C–N bond appears to be the primary step in the thermolysis of DNP. The T/Jump FT-IR analysis showed that CH₂O, NO₂, and NO are produced in larger amounts than CO₂ and HCN.

References

- [1] M. Farber, R.D. Srivastava, Proceedings of the 16th JANNAF Combustion Meeting, Monterey, CA, CPIA Publication No. 308, 1979, pp. 59–63.
- [2] R. Shaw, F.E. Walker, Estimated kinetics and thermochemistry of some initial unimolecular reactions in the thermal decomposition of HMX in the gas phase, *J. Phys. Chem.* 81 (25) (1977) 2572–2576.
- [3] W. Pan, J. Chang, Improvement of combustion property of double base propellant with *N,N'*-dinitropiperazine, *Guti Huojian Jishu* 20 (1) (1997) 36–40.
- [4] W. Pan, J. Chang, Influence of *N,N'*-dinitropiperazine on characteristics of composite modified double base propellant, in: Proceedings of the International Annual Conference of ICT27th (Energetic Materials), 1996, pp. 50.1–50.9.
- [5] Li Shangwen, Men Xiquan, Yang Wuquan, The effect of energetic additive, *N,N'*-dinitropiperazine (DNP) on properties of smokeless propellant, in: Proceedings of the International Annual Conference of ICT, 21st (Technol. Polym. Compd. Eng. Mater.), 1990, pp. 42/1–42/13.
- [6] T.B. Brill, Y. Oyumi, Thermal decomposition of energetic materials. 17. A relationship of molecular composition to HONO formation, *J. Phys. Chem.* 90 (1986) 6848–6853.
- [7] Y. Oyumi, T.B. Brill, Thermal decomposition of energetic materials. 22. The contrasting effects of pressure on the high-rate thermolysis of 34 energetic compounds, *Combust. Flame* 68 (1987) 209–216.
- [8] J.S. Murray, P.C. Redfern, J.M. Seminario, P. Politzer, Anomalous energy effects in some aliphatic and alicyclic aza-systems and their nitro derivatives, *J. Phys. Chem.* 94 (6) (1990) 2320–2327.
- [9] P. De, L.G. Jose, J. Ciller, On the use of AM1 and PM3 methods on energetic compounds, *Propell. Explos. Pyrotech.* 18 (1) (1993) 33–39.
- [10] Y. Yinon, NATO ASI Ser. C Liquid chromatography/mass spectrometric analysis of explosives: RDX adduct ions, *Chem. Phys. Energy Mater.* 309 (1990) 695–702.

- [11] Yu.Yu. Nikishev, I.S. Saifullin, I.F. Falyakhov, *Kinet. Katal.* 32 (3) (1991) 749.
- [12] G.V. Sitonina, B.L. Korsunskii, N.F. Pyamakov, et al., The kinetics of the thermal decomposition of *N,N'*-dinitropiperazine and 1,3-dinitro-1,3-diazacyclopentane, *Russ. Chem. Bull.* 28 (1979) 284–288.
- [13] S.M. Peiris, Richard, C. Mowrey, Craig A. Thompson, T.P. Russell, Computational and experimental infrared spectra of 1,4-dinitropiperazine and vibrational mode assignment. *J. Phys. Chem. A* 104 (39) 8898–8907 (2000) 10.1021.
- [14] T. Ozawa, A new method of analyzing thermogravimetric data, *Bull. Chem. Soc. Jpn.* 38 (1) (1965) 1881–1886.
- [15] J.H. Flynn, L.A. Wall, A quick, direct method for the determination of activation energy from thermogravimetric data, *Polymer Lett.* 4 (1966) 323–328.
- [16] S. Vyazovkin, C.A. Wight, Kinetics of thermal decomposition of cubic ammonium perchlorate, *Chem. Mater.* 11 (1999) 3386.
- [17] S. Vyazovkin, A unified approach to kinetic processing of nonisothermal data, *Int. J. Chem. Kinet.* 28 (1996) 95.
- [18] T. Zhang, R. Hu, Y. Xie, F. Li, The estimation of critical temperatures of thermal explosion for energetic materials using non-isothermal DSC, *Thermochim. Acta* 244 (1994) 171–176.
- [19] R. Hu, Z. Yang, Liang S Y., The determination of the most probable mechanism function and three kinetic parameters of exothermic decomposition reaction of energetic materials by a single non-isothermal DSC curve, *Thermochim. Acta* 123 (1988) 135–151.
- [20] C.F. Melius, in: S.N. Bulusu (Ed.), *Chemistry and Physics of Energetic Materials*, Kluwer Academic Press, Boston, 1990, pp. 43–49.
- [21] T.L. Boggs, in: K.K. Kuo, M. Summerfield (Eds.), *Fundamentals of Solid Propellant Combustion*, AIAA, New York, 1984, pp. 121–132.
- [22] A.J.B. Robertson, The thermal decomposition of explosives. Part II. Cyclotrim ethylene trinitramine and cyclotetram ethylenete trinitramine, *Trans. Faraday Soc.* 45 (1949) 85–98.
- [23] B. Suryanarayana, R.J. Graybush, J.R. Autera, Thermal degradation of secondary nitramines: a Nitrogen-15 tracer study of HMX (1,3,5,7-tetranitro-1,3,5,7-tetrazacyclooctane), *Chem. Ind. (Lond.)* (1967) 2177–2178.
- [24] B. Suryanarayana, R.J. Graybust, Proceedings of the 39th Congress on Industrial Chemistry, Brussels, Belgium, 1966.
- [25] K.V. Prabhakaran, S.R. Naidu, E.M. Kurian, X.R.D. Spectroscopic, Thermal-analysis studies on 3-nitro-1,2,4-triazole-5-one (Nto), *Thermochim. Acta* 241 (1994) 199–212.
- [26] S.R. Naidu, N.M. Bhide, K.V. Prabhakaran, E.M. Kurian, Thermal and spectroscopic studies on the decomposition of some aminoguanidine nitrates, *J. Therm. Anal.* (2006) 861–871.
- [27] J.D. Cosgrove, A.J. Owen, The thermal decomposition of 1,3,5-trinitrohexahydro-1,3,5-triazine (RDX). Part II. The effects of products, *Combust. Flame* 22 (1974) 13–18.